Environ Monit Assess (2023) 195:1525
https://doi.org/10.1007/s10661-023-12100-0

RESEARCH

Determination of landslide susceptibility with Analytic Hierarchy Process (AHP) and the role of forest ecosystem services on landslide susceptibility

Hasan Aksoy

Received: 11 August 2023 / Accepted: 6 November 2023 / Published online: 23 November 2023

Abstract The analysis of landslide susceptibility is a crucial tool in the mitigation and management of ecological and economic hazards. The number of studies examining how the form and durability of forest areas affect landslide susceptibility is very limited. This study was conducted in the Marmara region of northwestern Türkiye, where forested areas and industrial zones are intertwined and dense. The landslide susceptibility map was produced by Analytic Hierarchy Process (AHP) method. In the context of AHP, a total of 12 different variables were employed, namely lithology, slope, curvatures, precipitations, aspect, distance to fault lines, distance to streams, distance to roads, land use, soil, elevation, and Normalized Difference Vegetation Index (NDVI). The performance analysis of the landslide susceptibility map was conducted using the Receiver Operating Characteristics (ROC) curve method. The AUC value was computed (0.809) for the landslide susceptibility map generated by using the AHP technique. Forest type maps were used to analyze the impact of forests on landslide susceptibility. In terms of forest structure, 4 main criteria were determined: stand structure, development stage, crown closure, and stand age. Each criterion was analyzed with Geographic Information Systems (GIS) by overlaying it with the landslide susceptibility map of the study area. The results showed that the risk of landslides was lowest in forests with more than one tree species, mature, development stage and of (e) > 52 cm, and crown closure of 41%—70% (2).

Keywords Landslide susceptibility · AHP · Stand structure · Stand development stage · Crown closure · Stand age

H. Aksoy (✉)
Vocational School of Ayancık, Department of Forestry, Program of Forestry and Forest Products, Sinop University, Sinop, Türkiye
e-mail: haksoy@sinop.edu.tr

Introduction

Landslides are generally the downward and outward movement of slope materials, which are triggered by different factors such as earthquakes, melting snow, or heavy rain, and may also occur due to human activities (Guzzetti et al., 2012; Quevedo et al., 2022). Landslides are one of the most common geological hazards and can cause serious loss of life and property in disaster areas (Dai et al., 2002, 2023; Niu et al., 2021). Earthquakes, landslides, floods, erosion, drought, rock falls and avalanches are among the main natural disasters in Türkiye (Dalkes & Korkmaz, 2023; Ergünay, 2007). In recent years, researchers have focused on investigating the impact of forests on landslides, emphasizing that forests have an important preventive effect on landslide formation (Zhang et al., 2022).

Among terrestrial ecosystems, forest ecosystems have a very important role in terms of providing services such as carbon sequestration, carbon emission, water, natural disasters and regulation of energy cycles (Herold et al., 2019; Puliti et al., 2021). Forests have the role of providing stability of slopes with water retention (Ghestem et al., 2011; Grima et al., 2020) and preventing geological disasters such as erosion and landslides (Schmaltz et al., 2017; Kim & Park, 2021). Some studies have found that forests play a major role in reducing landslide susceptibility, soil moisture, and technical costs for landslide prevention (Dorren & Schwarz, 2016; Grima et al., 2020; Huang et al., 2021; Hwang et al., 2008; Li et al., 2022; Peduzzi, 2010). The fact that forest trees have differences such as root systems (Davoudi et al., 2004; Jamal & Mandal, 2016) has different effects on the landslide susceptibility of different forest forms (Dias et al., 2017; Moos et al., 2016). Especially natural forests have higher infiltration ability and soil retention effects compared to industrial plantations (Tosi, 2007; Zhang et al., 2022). Distinct tree species exhibit varying impacts on the occurrence of landslides. In shallow-rooted coniferous forest, which consists of a single species, slope stability is high at young ages, but decreases as it reaches maturity and causes different effects on landslides (Facelli & Temby, 2002). Identification of areas susceptible to landslides is important for taking measures to minimise economic losses, danger to life (Chen et al., 2014; Demir, 2019; Akinci & Yavuz Ozalp, 2021) and other adverse effects of landslides (Demir, 2019; Solaimani et al., 2013). Furthermore, landslide susceptibility mapping (LSM) assists planners, local authorities, and decision-makers in disaster planning (Erener et al., 2016; Akinci & Yavuz Ozalp, 2021). In conclusion, obtaining reliable landslide susceptibility maps using accurate data and novel techniques is of paramount importance for purposes such as the implementation of landslide mitigation measures (Corominas et al., 2014; Tien Bui et al., 2018). Various techniques are employed to create landslide susceptibility maps. Many researchers have determined landslide susceptibility using probabilistic models (Lee & Min, 2001; Cevik & Topal, 2003; Talaei et al., 2004; Lee & Dan, 2005; Clerici et al., 2006; Akgun & Türk, 2010; Talaei, 2014; Aghlmand et al., 2020; Akinci & Yavuz Ozalp, 2021). In addition, various machine learning algorithms methods were also employed to map landslide susceptibility, such as neuro-fuzzy (Bui et al., 2012; Pradhan et al., 2010; Tien Bui et al., 2018), artificial neural network (ANN) (Dou et al., 2015; Polykretis et al., 2015; Tien Bui et al., 2016a, b), random forest (RF) (Chen et al., 2018a, b; Trigila et al., 2015), decision trees (DT)(Al-Shabeeb et al., 2022; Hong et al., 2015; Tien Bui et al., 2018), support vector machines (SVM)(Al-Shabeeb et al., 2022; Chen et al., 2018a, b; Hong et al., 2016; Tien Bui et al., 2016a, b) and naive Bayes (Mabdeh et al., 2022; Tien Bui et al., 2012, 2018). Recently, Geographic Information Systems (GIS) have also been used by researchers in landslide susceptibility analysis. GIS can analyze all factors that cause landslide formation systematically and with high precision. GIS has recently been integrated with the Analytic Hierarchy Process (AHP) method in landslide susceptibility analysis (Saaty & Brandy, 2009; Zahedi, 1986). The AHP method, one of the multi-criteria evaluation methods, is based on the principle of sensitivity analysis by determining the degree of importance of the parameters that affect landslide formation relative to each other (Berber & Ceryan, 2023).

In this study, a landslide susceptibility map was created with the AHP method and the effect of the form and resilience of forest areas on landslide susceptibility was analyzed. A total of 12 criteria including lithology, slope, curvatures, precipitations, aspect, faultlines distance, stream distance, road distance, land use, soil, elevation, and NDVI were used to create the landslide susceptibility map. Stand structure, development stage, crown closure, and stand age were used as input to analyze the effects of forest areas on landslide susceptibility. Thus, it was tried to identify ways to ensure that the decisions to be taken and policies to be determined for the planning and management of forest ecosystems are also realized by landslide risk assessment and management.

Material and method

Material

Study area

The study was conducted within the administrative boundaries of the İnegöl Forest Management Directorate in İnegöl district of Bursa province, located in

the Marmara region of Türkiye. The study boundary is located between 29^0 0.40' – 29^0 0.20' north latitude and 39^0 0.50' – 40^0.10' east longitude. Of the 111,847.7 ha study area, 38% (42,502.126 ha) is forested area and 62% (69,345.574 ha) is non-forest area. Of the forest area, 71% (30,176,509 ha) is productive forest and 29% (12,325,616 ha) is degraded forest. The study area has a mild Marmara climate. The summer months are more similar to the Mediterranean climate, hot and less rainy. The winter months are cold and rainy. The average annual temperature is 12.4 °C. The average summer temperature is 21.9 °C and the average winter temperature is 2.3 °C (GDF, 2017). The location of the study area is shown in Fig. 1.

Dataset

The research was conducted in two primary phases. The initial step entails generating a map that depicts the susceptibility of landslides occurring within the designated study area. Subsequently, the subsequent step is to assess the influence of forests on the susceptibility to landslides. In the study, 12 variables were used to create the landslide susceptibility map. These are lithology, slope, curvature, rainfall, aspect, distance to fault lines, distance to streams, distance to roads, land use, soil, elevation, and NDVI. At this stage, the digital elevation model (DEM) was used to create the study area's, slope, curvatures, aspect, and elevation maps. The DEM was derived from ALOS-PALSAR satellite imagery acquired from EarthDATA. In addition, the NDVI map was generated using Landsat 8 OLI satellite imagery dated 27.08. 2022. Band 4 and band 5 were used to calculate NDVI from the Landsat satellite image. For the precipitations variable, fixed meteorological station data, DEM, and ArcGIS software inverse distance weighted (IDW) tool were used. OpenStreetMap vector data was used to generate the stream distance and road distance maps. Lithology, faultlines distance, and soil data were obtained from the official website of the General Directorate of Mineral Research and

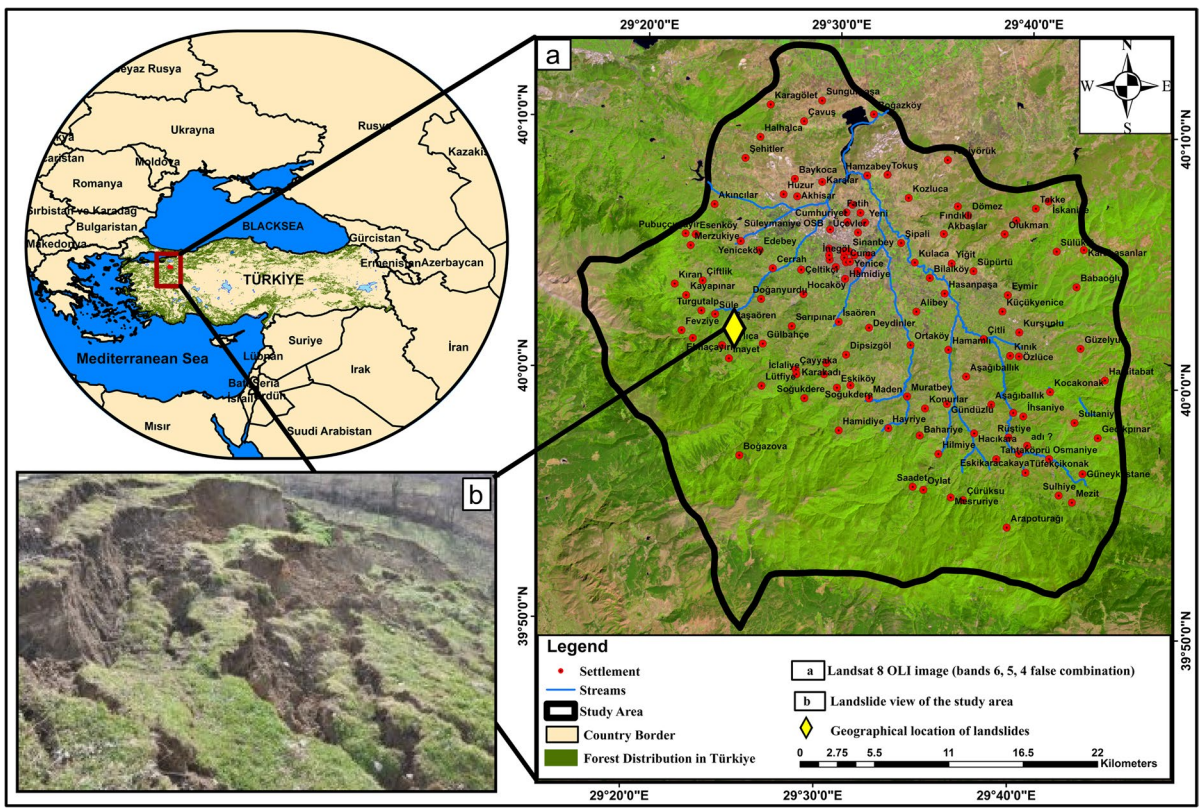

Fig. 1 Location of the study area

Exploration (GDMRE) (GDMRE, 2022). In addition, observational landslide inventories from GDMRE and observational and actual landslide inventory data from the Disaster and Emergency Management Presidency (AFAD, 2020) were used to assess the accuracy of the landslide susceptibility map. Finally, the land use map was created using Corine data from the National Land Cover Classification System (TOB, 2022) of the Ministry of Agriculture and Forestry. In the second stage of the analysis, a forest type map was used to investigate the impact of forests on landslide susceptibility. The forest type map is shown in Fig. 2 and the map series for the criteria used in landslide susceptibility analysis is shown in Fig. 3.

Method

In the study, the investigation of the impact of forests on landslide susceptibility was carried out in two stages. In the first stage, the landslide susceptibility map of the study area was obtained using the Analytic Hierarchy Process (AHP) multi-criteria decision-making method. In the second stage, the impact of forest types on landslide susceptibility was analyzed using the forest type map of the study area. The overall workflow diagram of the study is shown in Fig. 4.

Analytical Hierarchy Process (AHP) and landslide susceptibility analysis

The AHP method, one of the multi-criteria decision-making methods, was used to create the landslide susceptibility map of the study area. A total of 12 criteria including lithology, slope, curvatures, precipitations, aspect, faultlines distance, stream distance, road distance, land use, soil, elevation, and NDVI were used to create the landslide susceptibility map. AHP is a mathematical method that takes into account the importance levels of individuals and classes, evaluates quantitative and qualitative inputs together, and

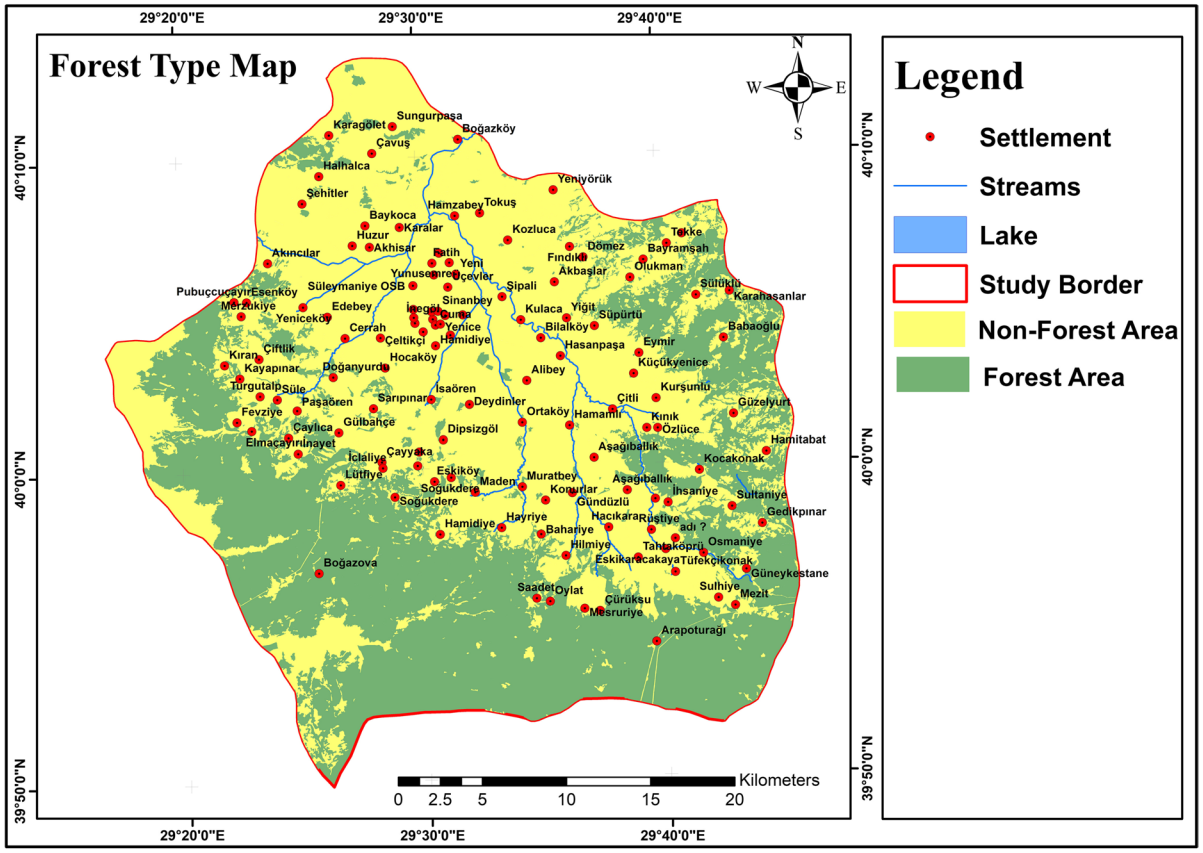

Fig. 2 Forest types map of the study area

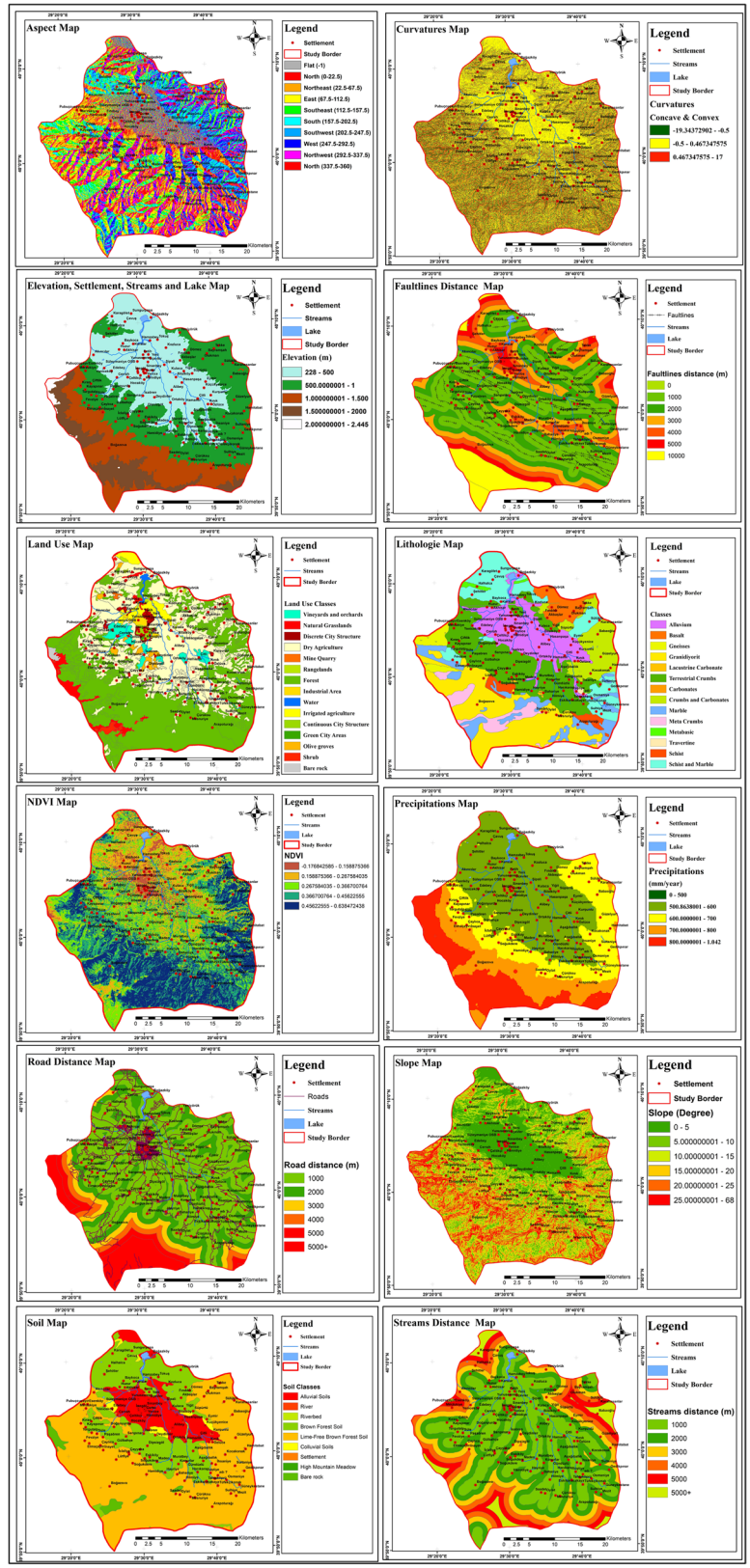

Fig. 3 Landslide susceptibility analysis criteria maps

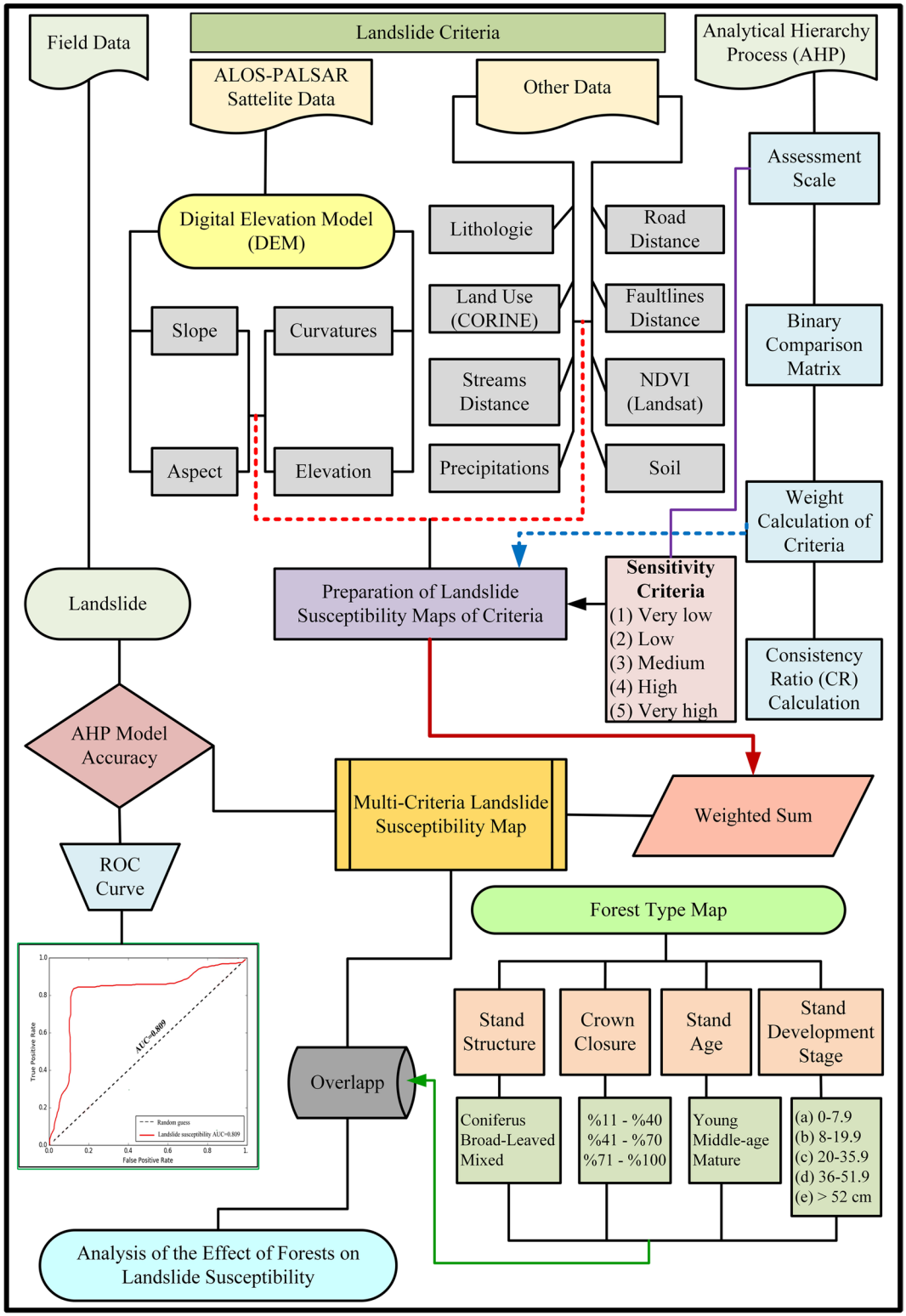

Fig. 4 Workflow diagram for the study

is based on the principle that the decision maker evaluates all alternatives together with all criteria and makes pairwise comparisons according to the relative importance of each other (Deniz & Çıtıroğlu, 2022; Gülenç & Bilgin, 2010). The AHP process consists of 4 main stages. In the first stage, the AHP evaluation scale is determined. The scale shown in Table 1 was used in this study (Saaty, 2012; Sivrikaya et al., 2022).

A pairwise comparison matrix for each criterion was created in the second stage using the AHP evaluation scale (Table 1). At this stage, determine which of the classes belonging to the criteria were the most important and the degree of importance of the class of interest compared to the other classes (Table 2). The effects of criteria on landslide susceptibility have been extensively discussed in many studies in the literature, and the importance levels of the criteria were determined based on these studies as references (Dai et al., 2001; Lee & Min, 2001; Çevik & Topal, 2003; Bragagnolo et al., 2020; Akinci & Yavuz Ozalp, 2021; Mabdeh et al., 2022; Al-Shabeeb et al., 2022). The lithologic map from GDMRE was digitized by clipping according to the study area. Four classes were identified on the digitized lithologies map; alluvium, crumbs, schist, and granidiorite. The crumbs class was selected as the most effective class on landslide susceptibility. Using the digital elevation model (DEM) obtained from the ALOS-PALSAR satellite image for the study area, a slope map of the study area was created in ArcGIS 10.7 software. Changes in slope gradients affect slope stability and landslide susceptibility (Al-Shabeeb et al., 2022). For the slope criterion, 6 classes were determined in degrees (0–5, 5–10, 10–15, 15–20, 2,0–25, and 25–68). The class with the highest degree of slope was scaled to be the riskiest class. For curvatures, 3 classes were determined as concave, flote slope, and convex. In this criterion, flat areas were scaled to be the least landslide-prone areas. The annual total precipitations map for the study area was produced using ArcGIS 10.7 software. Firstly, fixed meteorological station data for the study area were obtained from the official website of ClimateData (URL-1, 2023). Then, by randomly assigning points to the study area, the heights of the points were determined on the DEM. Based on the fixed meteorological station height and precipitation amount for the study area, the precipitation amounts of randomly assigned points were determined and the general precipitations map of the study area was created using the IDW command. Finally, the precipitations criterion was divided into five classes and made ready for analysis (500.86–600, 600–700, 700–800, 800–900, 900–1,042.25 mm). Aspect and elevation maps were also generated using ArcGIS 10.7 software, utilizing the DEM data. Aspect is the steepest downhill direction (Al-Shabeeb et al., 2022; Kadavi et al., 2018). For aspect, four classes were determined: North, South, East–West, and flat area. For elevation, five classes were defined (228–500, 500–1000, 1000–1500, 1500–2000, 2000–2445 m). The faultlines distance map of the study area was also created by digitizing the faultlines map obtained from GDMRE by clipping it according to the study area. Then the faultlines distance map was divided into 6 classes 1000, 2000, 3000, 4000, 5000, and 10,000 m Stream distance and road distance maps were also divided into 6 classes as in the faultlines distance criterion. The land use map is divided into 7 classes; bare rock, mine quarry, rangelands, grasslands, agriculture, vineyards, and settlement. The soil map of the study area was also created by digitizing the soil map obtained from GDMRE by clipping it according to the study

Table 1 The pairwise comparison scale in the AHP

Importance scale	Definitions of importance	Explanation
1	Equal	Two activities contribute equally to the goal
3	Moderate	Experience and judgment are slightly preferable to another
5	Strong	Experience and judgment are strongly preferable to another
7	Very Strong	Experience and judgment are very strongly preferable to another
9	Extreme	Experience and judgment are of the highest possible order of affirmation
2, 4, 6, 8	Intermediate	When you need to make a compromise

Table 2 AHP binary comparison matrix of criteria

Criteria	Classes	1	2	3	4	5	6	7	Criteria	Classes	1	2	3	4	5
Land use (Corine)	(1) Bare rock	1	2	3	4	5	6	7	Soil type	(1) Bare rock	1	2	3	4	5
	(2) Mine Quarry		1	2	3	4	5	7		(2) Alluvial		1	2	3	4
	(3) Rangelands			1	2	3	5	7		(3) Colluvial			1	2	3
	(4) Grasslands				1	3	5	7		(4) Settlement				1	3
	(5) Agriculture					1	2	3		(5) Forest Soil					1
	(6) Vineyards						1	2	Precipitations (mm)	(5) 900—1042.25	1	2	3	4	5
	(7) Settlement							1		(4) 800—900		1	2	3	4
Slope (Degree)	(1) 0—5	1	2	3	4	5	6			(3) 700—800			1	2	3
	(2) 5—10		1	2	3	4	5			(2) 600—700				1	3
	(3) 10—15			1	2	3	5			(1) 500.86—600					1
	(4) 15—20				1	3	5		Elevation (m)	(5) 2000—2445	1	2	3	4	5
	(5) 20—25					1	2			(4) 1500—2000		1	2	3	4
	(6) 25—68						1			(3) 1000—1500			1	2	3
Faultlines distance	(1) 1000 m	1	2	3	5	7	9			(2) 500—1000				1	3
	(2) 2000 m		1	3	5	7	9			(1) 228—500					1
	(3) 3000 m			1	3	5	7		NDVI	(1) -0.17—0.15	1	2	3	4	5
	(4) 4000 m				1	3	5			(2) 0.15—0.26		1	2	3	4
	(5) 5000 m					1	3			(3) 0.26—0.36			1	2	3
	(6) > 10,000 m						1			(4) 0.36—0.45				1	3
Road distance	(1) 1000 m	1	2	3	5	7	9			(5) 0.45—0.63					1
	(2) 2000 m		1	3	5	7	9		Aspect (Degree)	(1) North	1	2	3	4	
	(3) 3000 m			1	3	5	7			(2) South		1	2	3	
	(4) 4000 m				1	3	5			(3) East–West			1	2	
	(5) 5000 m					1	3			(4) Flat Areas				1	
	(6) > 10,000 m						1		Curva-tures	(1) Concave	1	2	3		
Stream distance	(1) 1000 m	1	2	3	5	7	9			(2) Flat Slope		1	2		
	(2) 2000 m		1	3	5	7	9			(3) Convex			1		
	(3) 3000 m			1	3	5	7		Lithologie	(1) Alluvium	1	2	3	4	
	(4) 4000 m				1	3	5			(2) Crumbs		1	2	3	
	(5) 5000 m					1	3			(3) Schist			1	2	
	(6) > 10,000 m						1			(4) Granodiorite				1	

boundary. Afterward, five classes were determined on the digital map (bare rock, alluvial, colluvial, settlement, and forest soil). Finally, a normalized difference vegetation index (NDVI) map was obtained using bands 4 and 5 of the Landsat 8 OLI satellite image. The bands were clipped according to the study area. Then the NDVI of the study area was calculated using the NDVI formula with the raster calculator command (Eq. 1). NDVI values range between -1 and + 1. Negative values in NDVI indicate areas devoid of water, snow, rocks, soil cover, and vegetation. Positive values indicate areas with high plant density. The NDVI map of the study area was also divided into 5 classes and made suitable for AHP analysis. After the classification of the criteria, the pairwise comparison matrix of each criterion was created using the AHP evaluation scale (Table 2).

$$NDVI = \frac{NIR - Red}{NIR + Red} \quad (1)$$

** NIR: Near infrared band, Red: Red band

In the third stage, weight calculations were made for the criteria. In the last stage, the consistency ratio (CR) was calculated to measure the consistency of the randomly generated importance matrix between the criteria (Eq. 3). The consistency ratio was obtained by dividing the consistency index value (CI) by the random index value (RI). The RI value is a constant coefficient depending on the number of criteria. The CI value was calculated using the sum of the mean consistency and the number of criteria (Eq. 2).

$$CI = \frac{\lambda max - n}{n - 1} \quad (2)$$

**λ_{max} is the largest or principal eigenvalue of the matrix, n number of criteria, CI consistency index, CR consistency ratio

$$CR = \frac{CI}{RI} \quad (3)$$

It is recommended that the consistency rate for AHP analysis should not exceed %10. If this ratio exceeds %10, it means that there is an inconsistency in the evaluation scale between the criteria and should be re-evaluated (Saaty & Brandy, 2009). After the weight calculations for the criteria were obtained in the AHP process, landslide susceptibility maps were created for each criterion. Finally, using the weight values of each criterion, the landslide susceptibility map of the study area was obtained using the "weight sum" command in ArcGIS software. The landslide susceptibility map was produced using the "Weighted Sum" tool in ArcGIS software. The landslide susceptibility map of the study area was divided into 5 classes by general classification. These classes were grouped as "very low", "low", "medium", "high" and "very high" using the natural break method in ArcGIS.

Accuracy assessment of landslide susceptibility map

The accuracy and suitability of landslide susceptibility maps can be evaluated by different performance analyses. The extent to which the produced susceptibility map can predict landslide areas is revealed by such analyses. In this study, Receiver Operating Characteristics (ROC) curve was used to analyze the accuracy of the landslide susceptibility map produced by the AHP method. The ROC curve is a curve with true positive (sensitivity) values on the vertical axis and false positive rate values on the horizontal axis for specified threshold values. These values in the ROC curve determine the accuracy of the model by distinguishing between positive and negative observations (Beguería, 2006). The line connecting the points (0,0) and (1,1) on the ROC curve is considered the reference line and the value of the area under this line is 0.5. The Area Under the Curve (AUC) value, defined as the area under the ROC curve, represents the result of the performance analysis. When the AUC is close to 1, it indicates an ideal model, and when it is close to 0.5, it indicates a model with very low accuracy (Fawcett, 2006; Sivrikaya & Küçük, 2022; Berber & Ceryan, 2023). The AUC value, or the quantitative measure of the quality of a model, is generally classified into five categories: poor (0.5–0.6), fair (0.6–0.7), good (0.7–0.8), very good (0.8–0.9), and excellent (0.9–1) (Akıncı & Akıncı, 2023; Chen et al., 2018a, b).

Impact of forests on landslide susceptibility

The forest type map of the study area was used to measure the effect of forests on landslide

susceptibility through the landslide susceptibility map of the study area. The forest type map was divided into four main groups: stand structure, stand development stage, crown closure, and stand age. Then stand structure the crown closure and stand age were divided into 3 separate classes, and the stand development stage into 5 separate classes for analysis (Table 3). Finally, the 4 criteria and subclasses obtained from the forest type map were overlapped with the landslide susceptibility map in ArcGIS software and descriptive statistical landslide susceptibility values of each class were obtained and interpreted.

Result

AHP and landslide susceptibility analysis

In the AHP process, class weights were determined for the criteria used in the analysis to produce a general landslide susceptibility map of the study area. Then, the consistency ratio (CR) was calculated to measure the consistency of the randomly generated importance matrix between the criteria. The weight and CR results for the criteria are shown in Table 4 and the weighted suitability maps of the criteria are shown in Fig. 5. The results show that the highest weight for the land use criterion was calculated for the bare rock class (0.34). The lowest was calculated for the settlement class (0.027). The highest weight for slope degrees was calculated for the 5—10 degree weight (0.372). In the faultlines, road, and stream distance criteria, the highest weight was calculated for the class at a distance of 1000 m (0.377). For the Soil criterion, the highest weight was calculated for the bare rock class (0.413), as for the land use class. The highest weight value for the precipitation criterion was calculated in the 900—1042.25 mm class (0.413). Within the Elevation criterion, the class with the highest elevation of the study area (2000–2445 m) was calculated with the highest weight ratio (0.413). For the NDVI criterion, the class with the lowest plant density was calculated as the highest weight ratio (0.413). The highest weight ratio was calculated for the North class in the Aspect criterion (0.466), the concave class in the curvatures criterion (0.535), and the alluvium class in the lithologie criterion (0.266).

The study shows that the CR rate for all criteria is below %10 (Table 4). These results show that the evaluation scale between the classes of each criterion is done consistently.

After the weighted susceptibility map for the criteria was created, the evaluation scale, weights, and consistency ratio (CR) of the 12 criteria used in the analysis were calculated to create the overall landslide susceptibility map of the study area (Table 5).

When Table 5 is examined, the criteria are listed in order of importance on landslide susceptibility. The most important and weighted criterion was determined as lithologie. Parameter weights according to the comparison matrix created by the AHP method; 0.204 for lithologie, 0.162 for slope, 0.150 for curvatures, 0.125 for precipitations, 0.093 for aspect, 0.072 for faultlines distance, 0.061 for stream distance, 0.043 for road distance, 0.032 for land use, 0.025 for soil, 0.019 for elevation, and finally it was calculated as 0.013 for NDVI. According to these results, the most effective parameters in the occurrence of landslides in the study area were determined as lithologie, slope, curvatures, and precipitations. The consistency ratio (CR) in the landslide susceptibility comparison matrix of the study area is below 10%. This result shows that the evaluation scale of the criteria used for landslide susceptibility is consistent and usable. The landslide susceptibility map was produced using the "Weighted Sum" tool in ArcGIS software. The landslide susceptibility map of the study area was divided into 5 classes by general classification. These classes

Table 3 Forest types map criteria and subclasses

Forest type map criteria				
Classes	Stand Structure	Devolopment Stage	Crown Closure	Stand Age
	Coniferous	(a) 0—7.9 cm	(1) %11—%40	Young
	Broad-Leaved	(b) 8—19.9 cm	(2) %41—%70	Middle-age
	Mixed	(c) 20—35.9 cm	(3) %71—%100	Mature
		(d) 36—51.9 cm		
		(e) > 52 cm		

Table 4 Weights and consistency ratios of all criteria and classes according to the AHP model

Criteria	Classes	Weights	CR	Criteria	Classes	Weights	CR
Land use (Corine)	(1) Bare rock	0.34	0.06	Soil type	(1) Bare rock	0.413	0.04
	(2) Mine Quarry	0.232			(2) Alluvial	0.259	
	(3) Rangelands	0.165			(3) Colluvial	0.159	
	(4) Grasslands	0.132			(4) Settlement	0.11	
	(5) Agriculture	0.063			(5) Forest Soil	0.058	
	(6) Vineyards	0.041		Precipitations (mm)	(5) 900—1042.25	0.413	0.04
	(7) Settlement	0.027			(4) 800—900	0.259	
Slope (Degree)	(1) 0—5	0.372	0.05		(3) 700—800	0.159	
	(2) 5—10	0.243			(2) 600—700	0.11	
	(3) 10—15	0.162			(1) 500.86—600	0.058	
	(4) 15—20	0.123		Elevation (m)	(5) 2000—2445	0.413	0.04
	(5) 20—25	0.06			(4) 1500—2000	0.259	
	(6) 25—68	0.039			(3) 1000—1500	0.159	
Faultlines distance	(1) 1000 m	0.377	0.08		(2) 500—1000	0.11	
	(2) 2000 m	0.297			(1) 228—500	0.058	
	(3) 3000 m	0.165		NDVI	(1) -0.17—0.15	0.413	0.04
	(4) 4000 m	0.088			(2) 0.15—0.26	0.259	
	(5) 5000 m	0.047			(3) 0.26—0.36	0.159	
	(6) > 10,000 m	0.026			(4) 0.36—0.45	0.11	
Road distance	(1) 1000 m	0.377	0.08		(5) 0.45—0.63	0.058	
	(2) 2000 m	0.297		Aspect (Degree)	(1) North	0.466	0.01
	(3) 3000 m	0.165			(2) South	0.277	
	(4) 4000 m	0.088			(3) East–West	0.161	
	(5) 5000 m	0.047			(4) Flat Areas	0.096	
	(6) > 10,000 m	0.026		Curva-tures	(1) Concave	0.535	0.009
Stream distance	(1) 1000 m	0.377	0.08		(2) Flat Slope	0.297	
	(2) 2000 m	0.297			(3) Convex	0.164	
	(3) 3000 m	0.165		Lithologie	(1) Alluvium	0.266	0.01
	(4) 4000 m	0.088			(2) Crumbs	0.377	
	(5) 5000 m	0.047			(3) Schist	0.161	
	(6) > 10,000 m	0.026			(4) Granidiorite	0.196	

were grouped as "very low", "low", "medium", "high" and "very high" and are shown in Fig. 6. The areal and proportional values of the sensitivity classes are shown in Table 6.

When the landslide susceptibility results of the study area are examined, it is seen that there is an area with very low landslide susceptibility at the rate of 3.8% (4,254.30 ha). The lowest class in the area and proportion is very high (3.8%—1,082.90 ha). The highest in terms of area and proportion is the medium class (57.65%—64,475.37 ha). After medium, the class with the highest sensitivity is low (33.46%—37,423.26 ha). Finally, the high class was ranked third in the area ranking of landslide susceptibility (4.12%—4,611.87 ha). When evaluated area-wise, it was determined that the study area is generally in low and medium landslide susceptibility. The general study area determined that the area is in a medium-risk position in terms of landslides.

AHP accuracy assessment of landslide susceptibility map

In the study, existing landslide spatial data overlapped with the produced landslide susceptibility map, and an accuracy assessment was performed. ROC curve

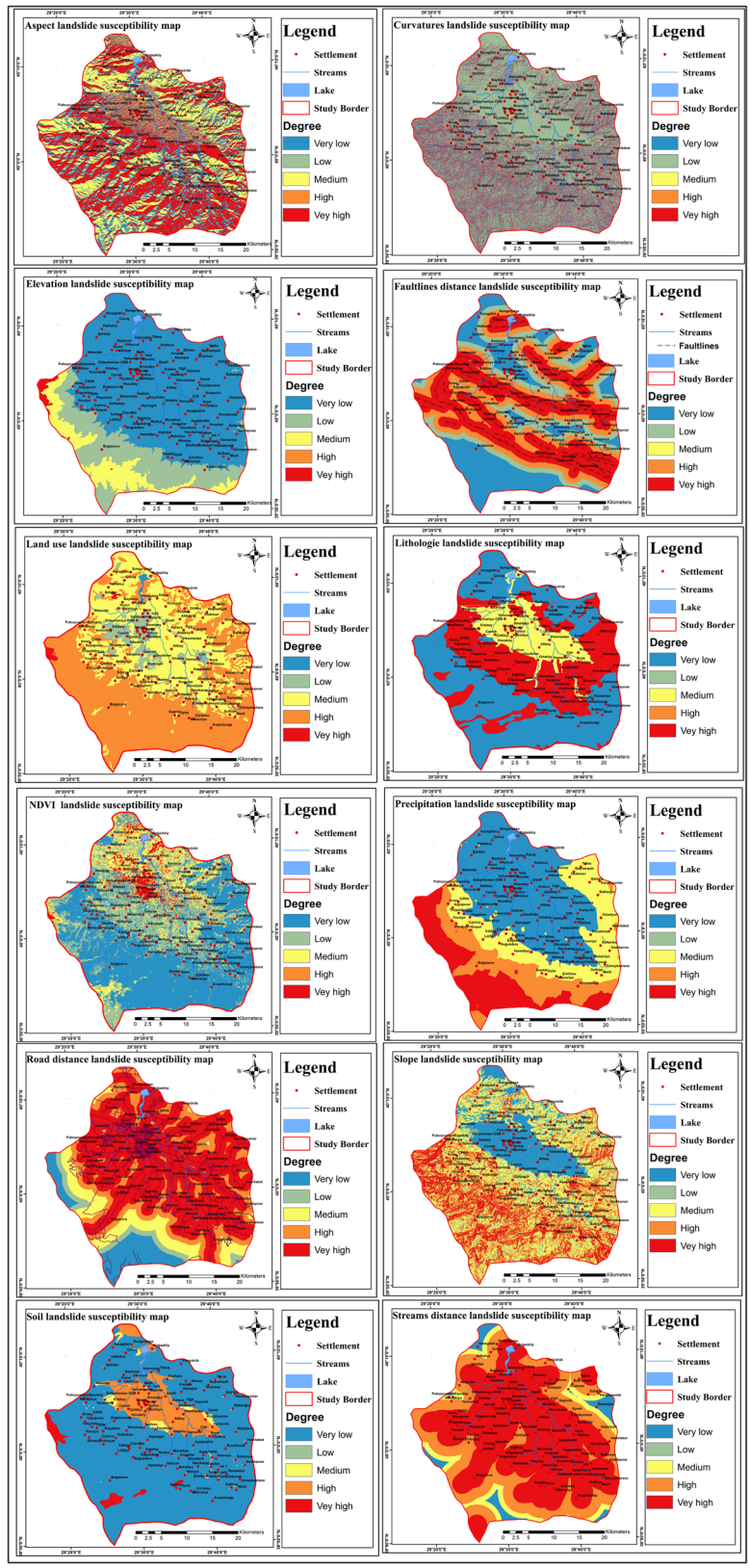

Fig. 5 Weighted sensitivity maps of criteria

Table 5 Evaluation scale, weights, and consistency ratios of all criteria according to the AHP

Criteria	Landslide sensitivity													
	Lithology	Slope	Curvatures	Precipitations	Aspect	Faultlines distance	Stream distance	Road distance	Land use	Soil	Elevation	Soil	Weights	CR
Lithology	1	2	2	3	4	4	4	4	5	5	5	9	0.204	0.092
Slope		1	2	2	3	3	4	5	5	5	5	7	0.162	
Curvatures			1	2	3	4	4	5	5	4	6	9	0.15	
Precipitations				1	2	3	4	5	5	6	7	7	0.125	
Aspect					1	2	3	4	5	5	5	7	0.093	
Faultlines distance						1	2	3	4	5	5	6	0.072	
Stream distance							1	2	3	5	5	7	0.061	
Road distance								1	2	3	4	5	0.043	
Land use									1	2	3	4	0.032	
Soil										1	2	3	0.025	
Elevation											1	2	0.019	
NDVI												1	0.013	

was used for accuracy assessment. After accuracy was performed using the ROC curve, AUC was plotted. When the AUC is close to 1, it indicates an ideal model, and when it is close to 0.5, it indicates a model with very low accuracy (Table 7) (Fawcett, 2006). The ROC curve for the study is shown in Fig. 7. The results showed that the model used was very good (AUC = 0.809).

Landslide susceptibility map rationality

The rationality of the landslide susceptibility map was assessed by considering the principle that "landslides should be located in areas of as high susceptibility as possible and very high susceptibility areas on the susceptibility map should be as small as possible" (Guo et al., 2021; Yavuz Ozalp et al., 2023). The rationality of the landslide susceptibility maps was assessed using the data in Table 8.

When Table 8 is analysed, as the landslide susceptibility increases, the frequency ratios also show an increasing trend. This shows that the landslide susceptibility map is reasonable. The fact that the highest ratio in the produced landslide susceptibility map is in the average landslide susceptibility (67.48%) and the frequency ratio increases from low landslide risk areas to high risk areas shows that the produced landslide susceptibility map is reasonable, applicable and rational.

Impact results of forests on landslide susceptibility

In the study, the landslide susceptibility map produced with AHP overlapped with the forest type map of the study area, and the results were analyzed. The forest map was divided into 4 main groups: stand structure, stand development stage, crown closure, and stand age. Descriptive statistics and areal values of landslide susceptibility for forest criteria are shown in Table 8.

When Table 9 is examined, it is seen that the broad-leaved class has the highest area in the stand structure criterion (76.66%). Then the highest area values belong to mixed (16.27%) and coniferous (7.07%) classes, respectively. The mean landslide susceptibility values for the stand structure criterion are 0.203, 0.217, and 0.220 for the coniferous, broad-leaved, and mixed classes, respectively. The maximum and minimum landslide susceptibility

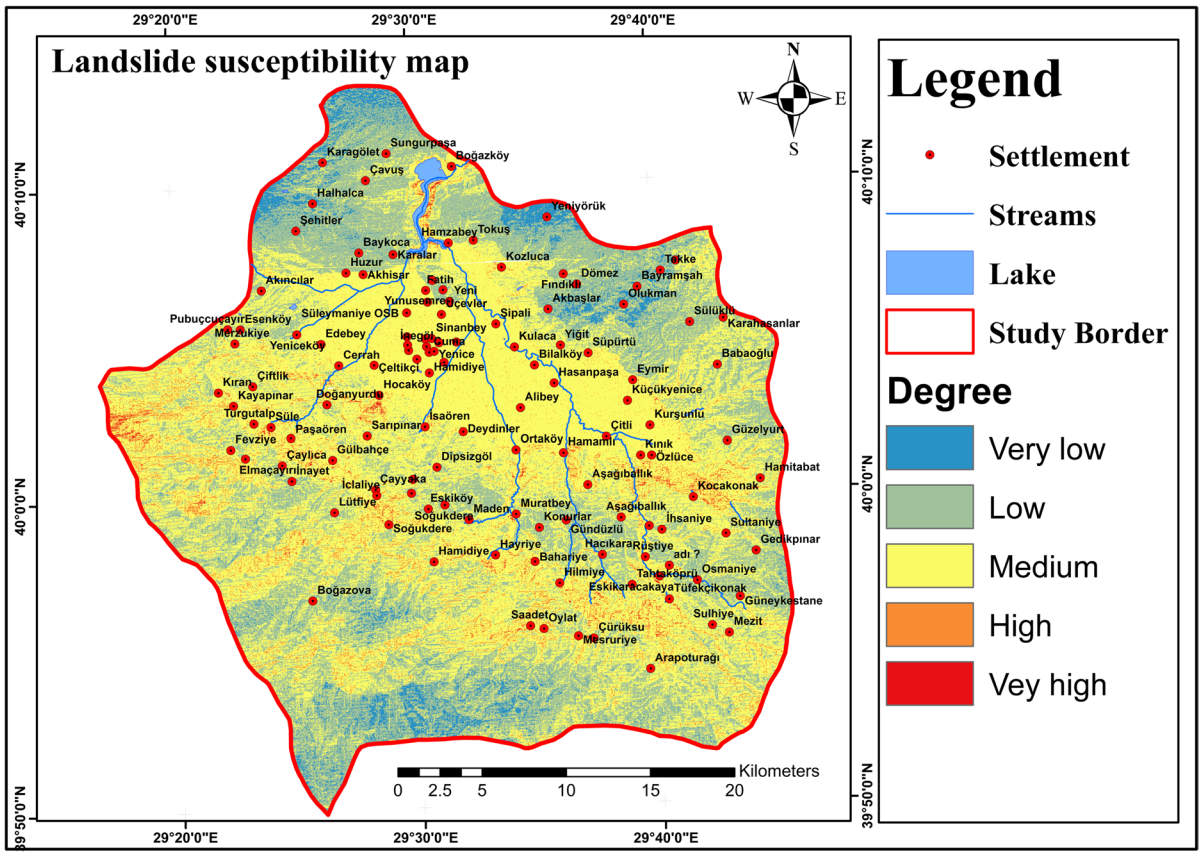

Fig. 6 Landslide susceptibility map of the study area

Table 6 Area values for landslide susceptibility levels

Value range	Landslide sensitivity level	Area (ha)	%
0.097—0.150	Very Low	4,254.30	3.80
0.150—0.204	Low	37,423.26	33.46
0.204—0.278	Medium	64,475.37	57.65
0.278—0.321	High	4,611.87	4.12
0.321—0.364	Very High	1,082.90	0.97
Total		111,847.70	100.00

Table 7 AHP model performance criteria

AUC (Area Under the Curve)	Model performance
0.9—1	Excellent
0.8—0.9	Very good
0.7—0.8	Good
0.6—0.7	Average
0.5—0.6	Poor

values for the stand structure criterion are 0.363 and 0.097, respectively. When the areal results for the stand development stage criterion in the study area are examined, it is seen that the highest area belongs to class "c" (38.05%). Then the highest area belongs to the "b" and "d" classes respectively (36.80%, 20.44%). The lowest area belongs to class "e" (1.21%). The mean landslide susceptibility values for the stand development stage criterion are 0.197, 0.210, 0.214, 0.217, and 0.221 for e, d, a, c, and b respectively. The maximum and minimum landslide susceptibility values for the stand development stage criterion are 0.363 and 0.097, respectively. It was determined that most of the forested area in the study area belonged to the "3" class for the crown closure criterion (82.79%). Then, it was determined that the most area was in the "2" class (15.66%), and finally, the "1" class was found to be 1.55%. The mean landslide susceptibility values for

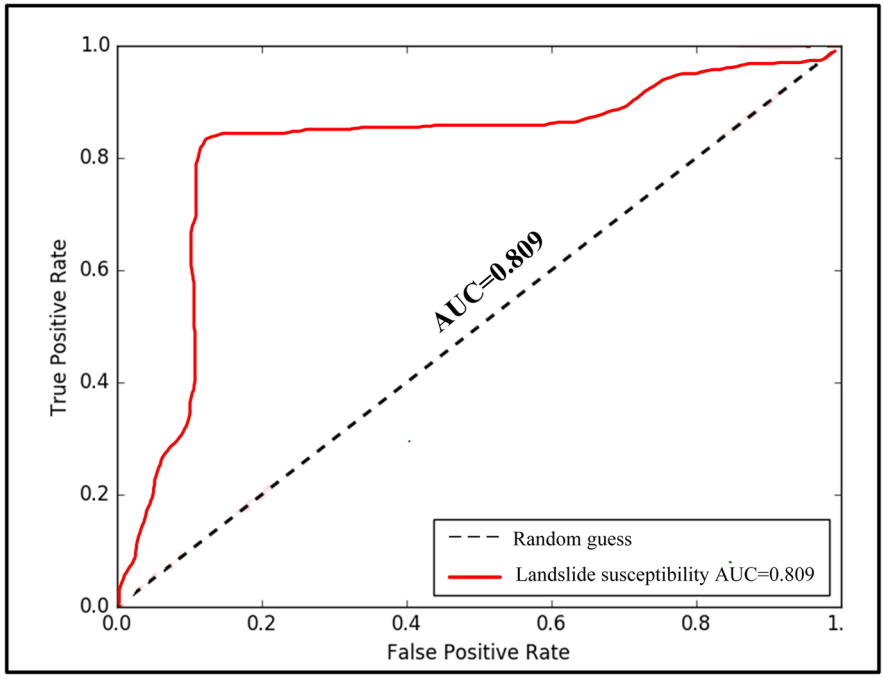

Fig. 7 ROC curve of landslide susceptibility obtained using AHP

Table 8 Landslide susceptibility map model results

Susceptibility level	Area percentage (%)	Landslide pixel	Landslide percentage (%)	Frequency ratio
Very low	3.83	124	0.118	0.0026
Low	33.72	29,511	28.042	0.0709
Moderate	57.93	71,032	67.497	0.0994
High	4.32	4461	4.239	0.0837
Very high	0.20	109	0.104	0.0452

Table 9 Descriptive statistics of landslide susceptibility for forest criteria

Criteria	Classes	Area (ha)	Area (%)	Min	Max	Mean	Std
Stand structure	Coniferous	3155.7395	7.07	0.114	0.330	0.203	0.036
	Broad-Leaved	34,195.631	76.66	0.097	0.363	0.217	0.037
	Mixed	7257.4878	16.27	0.097	0.326	0.220	0.036
Stand development stage	(a) 0—7.9	1562.3361	3.50	0.117	0.334	0.214	0.034
	(b) 8—19.9	16,417.752	36.80	0.097	0.363	0.221	0.036
	(c) 20—35.9	16,973.573	38.05	0.106	0.333	0.217	0.037
	(d) 36—51.9	9117.1868	20.44	0.101	0.337	0.210	0.037
	(e) > 52 cm	538.01054	1.21	0.133	0.257	0.197	0.026
Crown closure	(1)%11—%40	689.33527	1.55	0.114	0.330	0.206	0.035
	(2)%41—%70	6985.9431	15.66	0.109	0.337	0.212	0.038
	(3)%71—%100	36,933.58	82.79	0.097	0.363	0.218	0.037
Stand age	Young	21,696.517	48.64	0.097	0.363	0.217	0.037
	Middle-age	9472.0592	21.23	0.110	0.346	0.223	0.037
	Mature	13,440.282	30.13	0.101	0.337	0.213	0.037

the crown closure criterion are 0.206, 0.212, and 0.218 for classes 1, 2, and 3 respectively. The maximum and minimum landslide susceptibility values for the crown closure criterion are 0.363 and 0.097, respectively. Finally, the descriptive statistics of the stand age criterion landslide susceptibility showed that most areas were classified as young (48.64%). Then the largest area was calculated in the mature class (30.13%). The middle-age class, with an areal ratio of 21.23%, was found to be the class that occupied the least area in the stand-age criterion. The mean landslide susceptibility values for the stand age criterion are 0.217, 0.223, and 0.213 for the young, middle-age, and mature classes, respectively. The maximum and minimum landslide susceptibility values for the stand age criterion are 0.363 and 0.097, respectively. The landslide susceptibility map of the study border, forested area is shown in Fig. 8.

Discussion

The study was carried out in two main stages. In the first stage, a landslide susceptibility map of the study area was created using a total of twelve criteria (lithology, slope, curvatures, precipitations, aspect, faultlines distance, stream distance, road distance, land use, soil, elevation, and NDVI). The AHP method was used to create the landslide susceptibility map. The accuracy of the AHP model was verified by ROC. In the second stage, the effects of forests on landslide susceptibility were analyzed. Very few studies have specifically and systematically analyzed the effects of forests on landslide susceptibility. In this study, the effects of stand structure, stand development stage, crown closure, and stand age on landslide susceptibility of forest areas were analyzed.

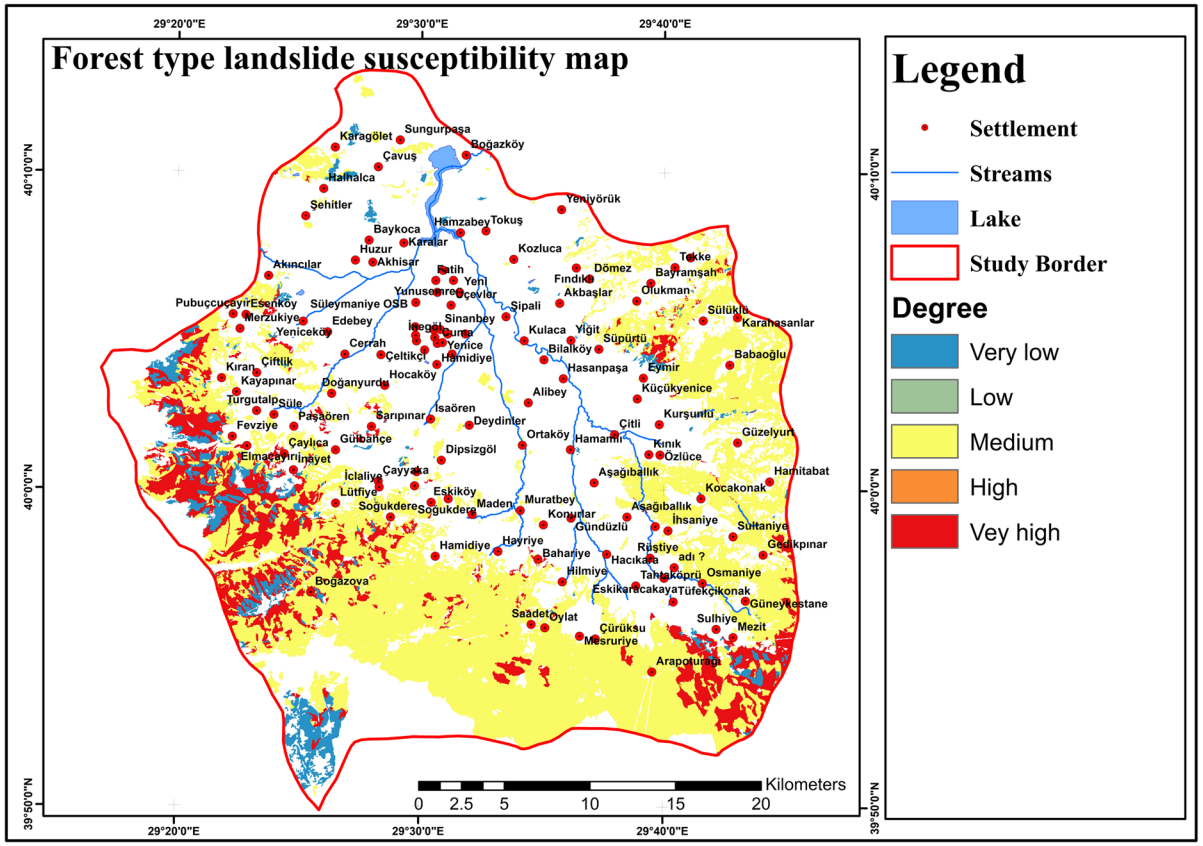

Fig. 8 Landslide susceptibility map of the forest area

The landslide susceptibility analysis using AHP

The criteria weights in the matrix created with the AHP method are; lithology 0.204, slope 0.162, curvatures 0.150, precipitation 0.125, aspect 0.093, distance to fault lines 0.072, stream distance 0.061, road distance 0.043, land use 0.032, soil 0.025, elevation 0.019 and NDVI 0.013 (Table 5). According to these results, the most effective criteria for landslide susceptibility in the study area were determined as lithologie, slope, curvatures, precipitations, and aspect. There are many studies in which landslide susceptibility maps are created with AHP. In the planned areas in Artvin city center, a landslide susceptibility map was obtained based on neighborhoods by using 5 different criteria with AHP, and it was revealed how much area in each neighborhood is susceptible to landslide events (Akıncı et al., 2015). Landslide susceptibility maps were produced for Sinop by using comparison matrices according to the weight values of the criteria with AHP (Çellek et al., 2015). Dalkes and Korkmaz (2023) created landslide susceptibility maps in the Akçaabat and Düzköy districts of Trabzon province by using 13 different spatial criteria with AHP and FR methods. When the criteria of the study were analyzed, the highest weight was created for the lithologie criterion. This is because different lithologic structures affect water transmission, shear stress, and susceptibility to sliding, and thus play an important role in landslide susceptibility. Similar to our study, Çellek (2013) emphasized that lithologie has a significant effect on landslide susceptibility as it is a criterion that controls cohesion. Another important criterion for landslide susceptibility is the slope. In the study, the slope was identified as the second most important determinant of landslide susceptibility (weight 0.162). As the slope increases, the balance of the escarpment material is disturbed and landslides are triggered. Gökçeoğlu and Ercanoğlu (2001) stated that slope is very effective on landslides. The third most important criterion is curvature. In Curvature, negative values indicate concave slopes and positive values indicate convex slopes. Concavity and convexity affect the direction of the flow of rainwater. Therefore, concave slopes are more susceptible to landslides. The main reason for this is that surface waters are more abundant than on convex slopes (Çellek, 2013). In the study, curvature was used as the 3rd most important criterion in landslide susceptibility with a weight ratio of 0.150. Another important criterion in landslide susceptibility is precipitations. Precipitations affect the stratification in the soil structure and thus soil strength, thus increasing landslide susceptibility. Therefore, the precipitations criterion was also considered the 4th most important criterion by weight (weight 0.125). Maturidi et al., (2021) stated in a study that more accurate results can be obtained by evaluating the precipitation criterion in landslide susceptibility over extreme precipitation. The 5th most important determinant in the study was aspect criteria (weight 0. 093). The aspect affects the response of slopes to atmospheric phenomena such as sunlight and precipitation. The landslide susceptibility of the slopes where there is more precipitation is higher and the heat energy from the sun causes water loss by transpiration and evaporation (evapotranspiration). In addition, the soil moisture of north-facing slopes is maintained for a long time after rainfall, which increases landslide susceptibility (Dalkes & Korkmaz, 2023). When the other criteria used in the study are evaluated, road works and locations close to the road increase landslide susceptibility (Bayrak & Ulukavak, 2009). Another factor influencing landslide susceptibility is vegetation cover (NDVI). Areas with no or sparse vegetation cover are more susceptible to landslides, while landslide susceptibility decreases in areas covered with vegetation as the effect of erosion decreases. Another criterion affecting landslide susceptibility is stream distance (0.061). The proximity to the valleys of rivers where surface water is collected causes ground movement and increases landslide susceptibility by saturating it with water. Due to the erosion of the lower parts of the river valleys, the slope balance deteriorates and it becomes susceptible to landslides (Dağ & Bulut, 2012). AHP model accuracy used in landslide susceptibility analysis was verified by the ROC curve. After validation was performed using the ROC curve, the area under the curve (AUC) was plotted. When AUC takes values close to 1, it indicates an ideal model, and when it takes values close to 0.5, it indicates a model with very low accuracy (Fawcett, 2006). The results showed that the model used was very good (AUC = 0.809).

Impact of forests on landslide susceptibility

Few studies have specifically investigated the impact of forests on landslide susceptibility. In this study, forest type maps and landslide susceptibility data were combined to analyze the effects of stand structure, stand development stage, crown closure, and stand age on landslide susceptibility. Different forest stands, stand development stages, crown closures, and stand ages were found to have different landslide susceptibility. The mean landslide susceptibility values of coniferous, broad-leaved, and mixed forest areas for the stand structure criterion are 0.203, 0.217, and 0.220, respectively. The results showed that mixed forest form was the most resistant to landslides, while coniferous forests were the least resistant. This is directly related to the root system. Because especially coniferous tree structures form a shallower root system compared to leafy tree species. The coniferous class is therefore less hardy than the broad-leaved class. Zhang et al., (2022) reported that coniferous forests are prone to landslides and have weaker landslide protection compared to broad-leaved forests. This is explained by the fact that the average tensile strength of the roots of coniferous tree species is weak and the improvement effect on the shear strength of the soil is relatively weak (Tan et al., 2019). Similar results were obtained with our study in terms of the effect of forest form on landslide susceptibility. In another study, it was stated that coniferous forests increase the risk of landslides due to the movement of thick soil layers with the effect of wind and precipitation due to their short root systems (Fusun et al., 2013). In general, it is thought that the use of mixed forest form in areas with landslide risk will provide the highest contribution to landslide susceptibility.

Another of the forest parameters is the stand development stage. Stand development stage was analyzed in 5 classes: (a) 0—7.9 cm, (b) 8—19.9 cm, (c) 20—35.9 cm, (d) 36—51.9 cm, and (e) > 52 cm. The mean landslide susceptibility values of classes a, b, c, d, and e are 0.214, 0.221, 0.217, 0.210, and 0.197, respectively (Table 8). The results generally revealed that as the stand development stage increases, landslide susceptibility decreases. This situation is explained by the fact that the root system in the low stage is not fully developed and the protective effect against landslides is low. As the stand development stage increases, the subsoil root system develops together with the stem and wraps the soil more tightly. Thus, it creates a high protection effect on landslides. Some studies also support this conclusion. Low-stage forests have fewer root systems and fewer soil and water conservation functions. In this period, landslides are likely to occur under the influence of heavy rainfall and the ability to protect against landslides is weak (Zhang et al., 2022). As the stand development stage increases, the ability to protect against landslides increases. This is explained by the fact that with the transition from young forests to middle-aged forests, the stability of the forest land increases, the root system gradually begins to develop, soil attachment strengthens and landslides do not occur easily (Šilhán, 2001; Sati & Sundiyal, 2007). When the landslide susceptibility of forests according to the crown closure criterion is analyzed, the average landslide susceptibilities for (1) 11%—40%, (2) 41%—70% and (3) 71%—100% are 0.206, 0.212 and 0.218, respectively. This is because in forests with low crown coverage, root, and stem development takes priority over height growth, and the root system is more likely to envelop and hold the soil. Therefore, it provides a more protective effect against landslides. Finally, the stand age criterion was analyzed in three classes: young, middle-age, and mature. The mean landslide susceptibility values for young, middle-age, and mature are 0.217, 0.223, and 0.213 respectively. The results showed that the landslide protection ability of forests of different age groups tended to increase and then decrease. This is explained by the fact that young forests have lower comprehensive productivity and lower vegetation density. As forests mature, their ability to protect against landslides increases. Similar results were obtained in some studies. Zhang et al., (2022) attribute this to the fact that as forests mature, the development of their roots, leaf density, the ability of the roots to rapidly absorb water from the soil, the development of the roots and their water infiltration capacity increase and thus contribute to the reduction of soil surface moisture. Thus, landslide resistance decreases and landslide risk decreases. This situation is similar to our results.

Conclusion

Landslides are one of the most dangerous and destructive natural disasters all over the world. Therefore, landslide detection is very important for politicians

and local people in a country. In addition, landslide susceptibility mapping helps land use planning and planners to make decisions for future development. A total of 12 criteria and the AHP method were used to determine landslide susceptibility. Then, the effect of forests on landslide susceptibility was analyzed in terms of stand structure, stand development stage, crown closure, and stand age. In general, it was determined that the mixed class was the most successful class in terms of landslide protection in the stand structure criterion. Older and thicker diameter stands were found to have a high impact on landslide susceptibility. In forest management, optimizing stand structure according to landslide susceptibility distribution is important for the integrity of economic, social, and ecological benefits. In addition, in terms of safety of life and property, it is recommended that landslide-sensitive areas in appropriate land use, selection and planning of tree forms that have a protective effect on landslide susceptibility, and not allowing construction in landslide-sensitive high areas are recommended as measures to be taken in landslide prevention. In further studies, it is important to examine landslide susceptibility in terms of tree species to determine which tree species would be more beneficial to be used in areas with high landslide risk in new afforestation.

Author contributions Hasan Aksoy designed the study, analyzed the satellite images, produced the maps, analyzed the data and wrote the manuscript.

Funding No funding was obtained for this study.

Data availability The authors do not have permission to share data.

Declarations

Ethics approval All authors have read, understood, and have complied as applicable with the statement on "Ethical responsibilities of Authors" as found in the Instructions for Authors.

Competing interests The authors declare no competing interests.

References

AFAD. (2020). Afet Yönetimi Kapsamında 2019 Yılına Bakış ve Doğa Kaynaklı Olay İstatistikleri, Afet ve Acil Durum Yönetimi Başkanlığı, https://www.afad.gov.tr/kurumlar/afad.gov.tr/e_Kutuphane/Kurumsal

Aghlmand, M., Onur, M. İ., & Talaei, R. (2020). Heyelan duyarlılık haritalarının üretilmesinde Analitik Hiyerarşi yönteminin ve Coğrafi Bilgi Sistemlerinin kullanımı. *Avrupa Bilim ve Teknoloji Dergisi*, 224–230. https://doi.org/10.31590/ejosat.araconf28

Akıncı, H. A., & Akıncı, H. (2023). Machine learning based forest fire susceptibility assessment of Manavgat district (Antalya), Turkey. *Earth Science Informatics, 16*(1), 397–414. https://doi.org/10.1007/s12145-023-00953-5

Akıncı, H., Özalp Yavuz, A., & Kılıçer, S. T. (2015). Coğrafi Bilgi Sistemleri ve AHP yöntemi kullanılarak planlı alanlarda heyelan duyarlılığının değerlendirilmesi: Artvin örneği. *Doğal Afetler ve Çevre Dergisi, 1*(1–2), 40–53. https://doi.org/10.21324/dacd.20952

Akinci, H., & Yavuz Ozalp, A. (2021). Landslide susceptibility mapping and hazard assessment in Artvin (Turkey) using frequency ratio and modified information value model. *Acta Geophysica, 69*(3), 725–745. https://doi.org/10.1007/s11600-021-00577-7

Akgun, A., & Türk, N. (2010). Landslide susceptibility mapping for Ayvalik (Western Turkey) and its vicinity by multicriteria decision analysis. *Environmental Earth Sciences, 61*, 595–611. https://doi.org/10.1007/s12665-009-0373-1

Al-Shabeeb, A. R., Al-Fugara, A. K., Khedher, K. M., Mabdeh, A. N., & Al-Adamat, R. (2022). Spatial mapping of landslide susceptibility in Jerash governorate of Jordan using genetic algorithm-based wrapper feature selection and bagging-based ensemble model. *Geomatics, Natural Hazards and Risk, 13*(1), 2252–2282. https://doi.org/10.1080/19475705.2022.2112096

Bayrak, T., & Ulukavak, M. (2009). Trabzon heyelanları. *Harita Teknolojileri Elektronik Dergisi, 1*(2), 20–30.

Beguería, S. (2006). Validation and evaluation of predictive models in hazard assessment and risk management. *Natural Hazards, 37*, 315–329. https://doi.org/10.1007/s11069-005-5182-6

Berber, S., & Ceryan, Ş. (2023). Güzelyalı-Lapseki (Çanakkale) arasındaki bölgenin heyelan duyarlılığının analitik hiyerarşi süreci yöntemiyle (AHP) değerlendirilmesi. *Balıkesir Üniversitesi Fen Bilimleri Enstitüsü Dergisi, 25*(1), 305–316. https://doi.org/10.25092/baunfbed.1208462

Bragagnolo, L., Da Silva, R. V., & Grzybowski, J. M. V. (2020). Artificial neural network ensembles applied to the mapping of landslide susceptibility. *CATENA, 184*, 104240. https://doi.org/10.1016/j.catena.2019.104240

Bui, D. T., Pradhan, B., Lofman, O., Revhaug, I., & Dick, O. B. (2012). Spatial prediction of landslide hazards in Hoa Binh province (Vietnam): A comparative assessment of the efficacy of evidential belief functions and fuzzy logic models. *CATENA, 96*, 28–40. https://doi.org/10.1016/j.catena.2012.04.001

Cevik, E., & Topal, T. (2003). GIS-based landslide susceptibility mapping for a problematic segment of the natural gas pipeline, Hendek (Turkey). *Environmental Geology, 44*, 949–962. https://doi.org/10.1007/s00254-003-0838-6

Chen, W., Li, W., Hou, E., Zhao, Z., Deng, N., Bai, H., & Wang, D. (2014). Landslide susceptibility mapping based on GIS and information value model for the Chencang District of Baoji, China. *Arabian Journal of Geosciences, 7*(11), 4499–4511. https://doi.org/10.1007/s12517-014-1369-z

Chen, W., Peng, J., Hong, H., Shahabi, H., Pradhan, B., Liu, J., ..., & Duan, Z. (2018a). Landslide susceptibility modelling using GIS-based machine learning techniques for Chongren County, Jiangxi Province, China. *Science of the Total Environment*, *626*, 1121–1135. https://doi.org/10.1016/j.scitotenv.2018.01.124

Chen, W., Pourghasemi, H. R., & Naghibi, S. A. (2018b). A comparative study of landslide susceptibility maps produced using support vector machine with different kernel functions and entropy data mining models in China. *Bulletin of Engineering Geology and the Environment, 77*, 647–664. https://doi.org/10.1007/s10064-017-1010-y

Corominas, J., van Westen, C., Frattini, P., Cascini, L., Malet, J. P., Fotopoulou, S., ..., & Smith, J. T. (2014). Recommendations for the quantitative analysis of landslide risk. *Bulletin of Engineering Geology and the Environment*, *73*, 209–263. https://doi.org/10.1007/s10064-013-0538-8

Çellek, S. (2013). Sinop-Gerze yöresinin heyelan duyarlılık analizi. Yayınlanmamış Doktora Tezi, Trabzon: Karadeniz Teknik Üniversitesi Fen Bilimleri Enstitüsü.

Çellek, S., Bulut, F., & Ersoy, H. (2015). AHP yöntemi'nin heyelan duyarlılık haritalarının üretilmesinde kullanımı ve uygulaması (Sinop ve Yakın Çevresi). *Jeoloji Mühendisliği Dergisi, 39*(2), 59–90. https://doi.org/10.24232/jeoloji-muhendisligi-dergisi.295366

Clerici, A., Perego, S., Tellini, C., & Vescovi, P. (2006). A GIS-based automated procedure for landslide susceptibility mapping by the conditional analysis method: the Baganza valley case study (Italian Northern Apennines). *Environmental Geology, 50*, 941–961. https://doi.org/10.1007/s00254-006-0264-7

Dağ, S., & Bulut, F. (2012). Coğrafi bilgi sistemleri tabanlı heyelan duyarlılık haritalarının hazırlanmasına bir örnek: Çayeli (Rize, KD Türkiye). *Jeoloji Mühendisliği Dergisi*, *36*(1), 35–62. https://dergipark.org.tr/en/pub/jmd/issue/28180/295921

Dai, F. C., Lee, C. F., & Ngai, Y. Y. (2002). Landslide risk assessment and management: An overview. *Engineering Geology, 64*(1), 65–87. https://doi.org/10.1016/S0013-7952(01)00093-X

Dai, F. C., Lee, C. F., Li, J. X. Z. W., & Xu, Z. W. (2001). Assessment of landslide susceptibility on the natural terrain of Lantau Island, Hong Kong. *Environmental Geology, 40*, 381–391. https://doi.org/10.1007/s002540000163

Dai, X., Zhu, Y., Sun, K., Zou, Q., Zhao, S., Li, W., ..., & Wang, S. (2023). Examining the spatially varying relationships between landslide susceptibility and conditioning factors using a geographical random forest approach: A case study in Liangshan, China. *Remote Sensing*, *15*(6), 1513. https://doi.org/10.3390/rs15061513

Dalkes, M., & Korkmaz, M. S. (2023). Analitik Hiyerarşi Süreci ve Frekans Oranı Yöntemlerinin Heyelan Duyarlılık Analizinde Karşılaştırılması: Trabzon İli Akçaabat ve Düzköy İlçeleri Örneği. *Doğal Afetler ve Çevre Dergisi, 9*(1), 16–38. https://doi.org/10.21324/dacd.1105000

Davoudi, M. H., Aghda, S. F., & Pour, G. S. A. (2004). Landslide stabilization by tree root reinforcement. WIT Transactions on Ecology and the Environment, 75. https://doi.org/10.2495/GEO040041

Demir, G. (2019). GIS-based landslide susceptibility mapping for a part of the North Anatolian Fault Zone between Reşadiye and Koyulhisar (Turkey). *CATENA, 183*, 104211. https://doi.org/10.1016/j.catena.2019.104211

Deniz, A., & Çıtıroğlu, H. K. (2022). Güneş enerjisi santral (GES) yapım yerlerinin CBS dayalı çok kriterli karar analizi ile belirlenmesi: Karabük örneği. *Geomatik, 7*(1), 17–25. https://doi.org/10.29128/geomatik.803200

Dias, A. S., Pirone, M., & Urciuoli, G. (2017). Review on the methods for evaluation of root reinforcement in shallow landslides. In Advancing Culture of Living with Landslides: Volume 2 Advances in Landslide Science (pp. 641–648). Springer International Publishing. https://doi.org/10.1007/978-3-319-53498-5_74

Dorren, L., & Schwarz, M. (2016). Quantifying the stabilizing effect of forests on shallow landslide-prone slopes. *Ecosystem-Based Disaster Risk Reduction and Adaptation in Practice* (255–270). https://doi.org/10.1007/978-3-319-43633-3_11

Dou, J., Yamagishi, H., Pourghasemi, H. R., Yunus, A. P., Song, X., Xu, Y., & Zhu, Z. (2015). An integrated artificial neural network model for the landslide susceptibility assessment of Osado Island, Japan. *Natural Hazards, 78*, 1749–1776. https://doi.org/10.1007/s11069-015-1799-2

Erener, A., Mutlu, A., & Düzgün, H. S. (2016). A comparative study for landslide susceptibility mapping using GIS-based multi-criteria decision analysis (MCDA), logistic regression (LR) and association rule mining (ARM). *Engineering Geology, 203*, 45–55. https://doi.org/10.1016/j.enggeo.2015.09.007

Ergünay, O. (2007). Türkiye'nin afet profili. *TMMOB Afet Sempozyumu Bildiriler Kitabı, 5*(7), 1–14.

Facelli, J. M., & Temby, A. M. (2002). Multiple effects of shrubs on annual plant communities in arid lands of South Australia. *Austral Ecology, 27*(4), 422–432. https://doi.org/10.1046/j.1442-9993.2002.01196.x

Fawcett, T. (2006). An introduction to ROC analysis. *Pattern Recognition Letters, 27*(8), 861–874. https://doi.org/10.1016/j.patrec.2005.10.010

Fusun, S., Jinniu, W., Tao, L., Yan, W., Haixia, G., & Ning, W. (2013). Effects of different types of vegetation recovery on runoff and soil erosion on a Wenchuan earthquake-triggered landslide, China. *Journal of Soil and Water Conservation, 68*(2), 138–145. https://doi.org/10.2489/jswc.68.2.138

GDF. (2017). General directorate of forestry, İnegöl forest management plan 2017–2027. Bursa forest regional directorate, Ankara: GDF (2017).

GDMRE. (2022). General directorate of mineral research and exploration. https://www.mta.gov.tr/v3.0/hizmetler/

Ghestem, M., Sidle, R. C., & Stokes, A. (2011). The influence of plant root systems on subsurface flow: Implications for slope stability. *BioScience, 61*(11), 869–879. https://doi.org/10.1525/bio.2011.61.11.6

Gökçeoğlu, C., & Ercanoğlu, M. (2001). Heyelan duyarlılık haritalarının hazırlanmasında kullanılan parametrelere ilişkin belirsizlikler. *Yerbilimleri, 22*(23), 189–206.

Grima, N., Edwards, D., Edwards, F., Petley, D., & Fisher, B. (2020). Landslides in the Andes: Forests can provide cost-effective landslide regulation services. *Science of the Total Environment, 745*, 141128. https://doi.org/10.1016/j.scitotenv.2020.141128

Guo, X., Fu, B., Du, J., Shi, P., Chen, Q., & Zhang, W. (2021). Applicability of susceptibility model for rock and loess earthquake landslides in the eastern Tibetan plateau. *Remote Sensing, 13*(13), 2546. https://doi.org/10.3390/rs13132546

Guzzetti, F., Mondini, A. C., Cardinali, M., Fiorucci, F., Santangelo, M., & Chang, K. T. (2012). Landslide inventory maps: New tools for an old problem. *Earth-Science Reviews, 112*(1–2), 42–66. https://doi.org/10.1016/j.earscirev.2012.02.001

Gülenç, İF., & Bilgin, G. A. (2010). Yatırım kararları için bir model önerisi: AHP Yöntemi-A model proposal for ınvestment decısıons: AHP method. *Öneri Dergisi, 9*(34), 97–107.

Herold, M., Carter, S., Avitabile, V., Espejo, A. B., Jonckheere, I., Lucas, R., ..., & De Sy, V. (2019). The role and need for space-based forest biomass-related measurements in environmental management and policy. *Surveys in Geophysics*, *40*, 757–778. https://doi.org/10.1007/s10712-019-09510-6

Hong, H., Pradhan, B., Jebur, M. N., Bui, D. T., Xu, C., & Akgun, A. (2016). Spatial prediction of landslide hazard at the Luxi area (China) using support vector machines. *Environmental Earth Sciences, 75*, 1–14. https://doi.org/10.1007/s12665-015-4866-9

Hong, H., Pradhan, B., Xu, C., & Bui, D. T. (2015). Spatial prediction of landslide hazard at the Yihuang area (China) using two-class kernel logistic regression, alternating decision tree and support vector machines. *CATENA, 133*, 266–281. https://doi.org/10.1016/j.catena.2015.05.019

Huang, G., Zheng, M., & Peng, J. (2021). Effect of vegetation roots on the threshold of slope instability induced by rainfall and runoff. *Geofluids, 2021*, 1–19. https://doi.org/10.1155/2021/6682113

Hwang, T., Kang, S., Kim, J., Kim, Y., Lee, D., & Band, L. (2008). Evaluating drought effect on MODIS Gross Primary Production (GPP) with an eco-hydrological model in the mountainous forest, East Asia. *Global Change Biology, 14*(5), 1037–1056. https://doi.org/10.1111/j.1365-2486.2008.01556.x

Jamal, M., & Mandal, S. (2016). Monitoring forest dynamics and landslide susceptibility in Mechi-Balason interfluves of Darjiling Himalaya, West Bengal using forest canopy density model (FCDM) and Landslide Susceptibility Index model (LSIM). *Modeling Earth Systems and Environment, 2*, 1–17. https://doi.org/10.1007/s40808-016-0243-2

Kadavi, P. R., Lee, C. W., & Lee, S. (2018). Application of ensemble-based machine learning models to landslide susceptibility mapping. *Remote Sensing, 10*(8), 1252. https://doi.org/10.3390/rs10081252

Kim, H. G., & Park, C. Y. (2021). Landslide susceptibility analysis of photovoltaic power stations in Gangwon-do, Republic of Korea. *Geomatics, Natural Hazards and Risk, 12*(1), 2328–2351. https://doi.org/10.1080/19475705.2021.1950219

Lee, S., & Dan, N. T. (2005). Probabilistic landslide susceptibility mapping in the Lai Chau province of Vietnam: Focus on the relationship between tectonic fractures and landslides. *Environmental Geology, 48*, 778–787. https://doi.org/10.1007/s00254-005-0019-x

Lee, S., & Min, K. (2001). Statistical analysis of landslide susceptibility at Yongin, Korea. *Environmental Geology, 40*, 1095–1113. https://doi.org/10.1007/s002540100310

Li, P., Xiao, X., Wu, L., Li, X., Zhang, H., & Zhou, J. (2022). Study on the shear strength of root-soil composite and root reinforcement mechanism. *Forests, 13*(6), 898. https://doi.org/10.3390/f13060898

Mabdeh, A. N., Al-Fugara, A. K., Ahmadlou, M., Al-Adamat, R., & Al-Shabeeb, A. R. (2022). GIS-based landslide susceptibility assessment and mapping in Ajloun and Jerash governorates in Jordan using genetic algorithm-based ensemble models. *Acta Geophysica, 70*(3), 1253–1267. https://doi.org/10.1007/s11600-022-00767-x

Maturidi, A. M. A. M., Kasim, N., Taib, K. A., & Azahar, W. N. A. W. (2021). Rainfall-induced landslide thresholds development by considering different rainfall parameters: A review. *Journal of Ecological Engineering, 22*(10), 85–97. https://doi.org/10.12911/22998993/142183

Moos, C., Bebi, P., Graf, F., Mattli, J., Rickli, C., & Schwarz, M. (2016). How does forest structure affect root reinforcement and susceptibility to shallow landslides? *Earth Surface Processes and Landforms, 41*(7), 951–960. https://doi.org/10.1002/esp.3887

Niu, C., Zhang, H., Liu, W., Li, R., & Hu, T. (2021). Using a fully polarimetric SAR to detect landslide in complex surroundings: Case study of 2015 Shenzhen landslide. *ISPRS Journal of Photogrammetry and Remote Sensing, 174*, 56–67. https://doi.org/10.1016/j.isprsjprs.2021.01.022

Peduzzi, P. (2010). Landslides and vegetation cover in the 2005 North Pakistan earthquake: A GIS and statistical quantitative approach. *Natural Hazards and Earth System Sciences, 10*(4), 623–640. https://doi.org/10.5194/nhess-10-623-2010

Polykretis, C., Ferentinou, M., & Chalkias, C. (2015). A comparative study of landslide susceptibility mapping using landslide susceptibility index and artificial neural networks in the Krios River and Krathis River catchments (northern Peloponnesus, Greece). *Bulletin of Engineering Geology and the Environment, 74*, 27–45. https://doi.org/10.1007/s10064-014-0607-7

Pradhan, B., Sezer, E. A., Gokceoglu, C., & Buchroithner, M. F. (2010). Landslide susceptibility mapping by neuro-fuzzy approach in a landslide-prone area (Cameron Highlands, Malaysia). *IEEE Transactions on Geoscience and Remote Sensing, 48*(12), 4164–4177.

Puliti, S., Breidenbach, J., Schumacher, J., Hauglin, M., Klingenberg, T. F., & Astrup, R. (2021). Above-ground biomass change estimation using national forest inventory data with Sentinel-2 and Landsat. *Remote Sensing of Environment, 265*, 112644. https://doi.org/10.1016/j.rse.2021.112644

Quevedo, R. P., Maciel, D. A., Uehara, T. D. T., Vojtek, M., Renno, C. D., Pradhan, B., ... ,& Pham, Q. B. (2022). Consideration of spatial heterogeneity in landslide susceptibility mapping using geographical random forest model. *Geocarto International*, 37:25, 8190–8213, https://doi.org/10.1080/10106049.2021.1996637

Sati, S. P., & Sundiyal, Y. P. (2007). Role of some tree species in slope instability. *Himalayan Geology, 28*(1), 75–78.

Saaty, T. L. (2012). *Decision making for leaders: The analytic hierarchy process for decisions in a complex world* (Third, Revised). RWS Publications.

Saaty, T. L., & Brandy, C. (2009). *The encyclicon, volume 2: a dictionary of complex decisions using the analytic network process*. Pittsburgh, Pennsylvania: RWS Publications.

Schmaltz, E. M., Steger, S., & Glade, T. (2017). The influence of forest cover on landslide occurrence explored with spatio-temporal information. *Geomorphology, 290*, 250–264. https://doi.org/10.1016/j.geomorph.2017.04.024

Šilhán, K. (2001). A new tree-ring-based index for the expression of spatial landslide activity and the assessment of landslide hazards. *Geomatics Natural Hazards and Risk, 12*(1), 3409–3428. https://doi.org/10.1080/19475705.2021.2011790

Sivrikaya, F., & Küçük, Ö. (2022). Modeling forest fire risk based on GIS-based analytical hierarchy process and statistical analysis in Mediterranean region. *Ecological Informatics, 68*, 101537. https://doi.org/10.1016/j.ecoinf.2021.101537

Sivrikaya, F., Özcan, G. E., Enez, K., & Sakici, O. E. (2022). Comparative study of the analytical hierarchy process, frequency ratio, and logistic regression models for predicting the susceptibility to Ips sexdentatus in crimean pine forests. *Ecological Informatics, 71*, 101811. https://doi.org/10.1016/j.ecoinf.2022.101811

Solaimani, K., Mousavi, S. Z., & Kavian, A. (2013). Landslide susceptibility mapping based on frequency ratio and logistic regression models. *Arabian Journal of Geosciences, 6*, 2557–2569. https://doi.org/10.1007/s12517-012-0526-5

Talaei, R. (2014). Landslide susceptibility zonation mapping using logistic regression and its validation in Hashtchin Region, northwest of Iran. *Journal of the Geological Society of India, 84*(1), 68–86. https://doi.org/10.1007/s12594-014-0111-5

Talaei, R., Ghayoumian, J., Akbarzadeh, E. A., & Shariat Jafari, M. (2004). Study on effective factor causing landslide in South West of Khalkhal Region.

Tan, H., Chen, F., Chen, J., & Gao, Y. (2019). Direct shear tests of shear strength of soils reinforced by geomats and plant roots. *Geotextiles and Geomembranes, 47*(6), 780–791. https://doi.org/10.1016/j.geotexmem.2019.103491

Tien Bui, D., Pham, B. T., Nguyen, Q. P., & Hoang, N. D. (2016a). Spatial prediction of rainfall-induced shallow landslides using hybrid integration approach of least-squares support vector machines and differential evolution optimization: A case study in Central Vietnam. *International Journal of Digital Earth, 9*(11), 1077–1097. https://doi.org/10.1080/17538947.2016.1169561

Tien Bui, D., Tuan, T. A., Klempe, H., Pradhan, B., & Revhaug, I. (2016b). Spatial prediction models for shallow landslide hazards: A comparative assessment of the efficacy of support vector machines, artificial neural networks, kernel logistic regression, and logistic model tree. *Landslides, 13*, 361–378. https://doi.org/10.1007/s10346-015-0557-6

Tien Bui, D., Pradhan, B., Lofman, O., & Revhaug, I. (2012). Landslide susceptibility assessment in vietnam using support vector machines, decision tree, and Naive Bayes Models. *Mathematical Problems in Engineering*, *2012*. https://doi.org/10.1155/2012/974638

Tien Bui, D., Shahabi, H., Shirzadi, A., Chapi, K., Alizadeh, M., Chen, W., ..., & Tian, Y. (2018). Landslide detection and susceptibility mapping by airsar data using support vector machine and index of entropy models in cameron highlands, malaysia. *Remote Sensing*, *10*(10), 1527. https://doi.org/10.3390/rs10101527

TOB. (2022). Tarım ve Orman Bakanlığı, Corine projesi arazi kullanımı sınıflandırması. https://corine.tarimorman.gov.tr/corineportal/

Tosi, M. (2007). Root tensile strength relationships and their slope stability implications of three shrub species in the Northern Apennines (Italy). *Geomorphology, 87*(4), 268–283. https://doi.org/10.1016/j.geomorph.2006.09.019

Trigila, A., Iadanza, C., Esposito, C., & Scarascia-Mugnozza, G. (2015). Comparison of Logistic Regression and Random Forests techniques for shallow landslide susceptibility assessment in Giampilieri (NE Sicily, Italy). *Geomorphology, 249*, 119–136. https://doi.org/10.1016/j.geomorph.2015.06.001

URL-1. (2023). https://en.climate-data.org/

Yavuz Ozalp, A., Akinci, H., & Zeybek, M. (2023). Comparative analysis of tree-based ensemble learning algorithms for landslide susceptibility mapping: A case study in Rize, Turkey. *Water, 15*(14), 2661. https://doi.org/10.3390/w15142661

Zahedi, F. (1986). The analytic hierarchy process—a survey of the method and its applications. *İnterfaces, 16*(4), 96–108. https://doi.org/10.1287/inte.16.4.96

Zhang, Y., Shen, C., Zhou, S., & Luo, X. (2022). Analysis of the influence of forests on landslides in the Bijie area of Guizhou. *Forests, 13*(7), 1136. https://doi.org/10.3390/f13071136